The 6dF Galaxy Survey: Mass and Motions in the Local Universe

Matthew Colless, Heath Jones, and Lachlan Campbell

Research School of Astronomy & Astrophysics, The Australian National University, Cotter Road, Weston Creek, ACT 2611, Australia

Daniel Burkey and Andy Taylor

Institute for Astronomy, University of Edinburgh, Royal Observatory, Blackford Hill, Edinburgh EH9 3HJ, U.K.

Will Saunders

Anglo-Australian Observatory, P.O. Box 296, Epping, NSW 1710, Australia

Abstract. The 6dF Galaxy Survey will provide 167 000 redshifts and about 15000 peculiar velocities for galaxies over most of the southern sky out to about $cz = 30000\,\mathrm{km\,s^{-1}}$. The survey is currently almost half complete, with the final observations due in mid-2005. An initial data release was made public in December 2002; the first third of the dataset will be released at the end of 2003, with the remaining thirds being released at the end of 2004 and 2005. The status of the survey, the survey database and other relevant information can be obtained from the 6dFGS web site at http://www.mso.anu.edu.au/6dFGS.

In terms of constraining cosmological parameters, combining the 6dFGS redshift and peculiar velocity surveys will allow us to: (1) break the degeneracy between the redshift-space distortion parameter $\beta = \Omega_m^{0.6}/b$ and the galaxy-mass correlation parameter r_g; (2) measure the four parameters A_g, Γ, β and r_g with precisions of between 1% and 3%; (3) measure the variation of r_g and b with scale to within a few percent over a wide range of scales.

1. The Survey

The 6dF Galaxy Survey (6dFGS) is designed to be the first of a new generation of combined redshift and velocity surveys ($z+v$-surveys). It consists of both a redshift survey of the local universe and a peculiar velocity survey using D_n–σ distances (Parker, Colless, & Mamon 1997a,b; Wakamatsu et al. 2003). The primary redshift survey sample is drawn from the 2MASS Extended Source Catalog (XSC), but also includes other 'interesting' source samples.

The survey covers the whole of southern sky excluding the region within $10°$ of the Galactic plane (i.e. $|b| > 10°$), an area of $17000\,\mathrm{deg^2}$. The primary z-survey sample comprises 2MASS galaxies down to $K_{tot} < 12.75$; these total magnitudes are estimated from the isophotal K_{20} magnitudes and surface brightness profile information given in the 2MASS XSC (Jarrett et al. 2000a,b). This primary sample is supplemented by secondary samples selected from the 2MASS and SuperCosmos catalogs that complete the combined sample down to limits of

180

Table 1.   The 6dFGS target samples.

Sample	Priority	Total	Sampling
2MASS $K_s < 12.75$	8	113988	94.1%
2MASS $H < 13.05$	6	3283	91.8%
2MASS $J < 13.75$	6	2008	92.7%
SuperCosmos $r_F < 15.7$	6	9199	94.9%
SuperCosmos $b_J < 17.0$	6	9749	93.8%
Shapley	6	939	85.7%
ROSAT All-Sky Survey	6	2913	91.7%
HIPASS $(> 4\sigma)$	6	821	85.5%
IRAS FSC	6	10707	94.9%
Denis $J < 14$	5	1505	93.2%
Denis $I < 15$	5	2017	61.7%
2MASS AGN	4	2132	91.7%
Hamburg-ESO Survey	4	3539	90.6%
NOAO-VLA Sky Survey	4	4334	87.6%
Total		167134	93.3%

$H = 13.05$, $J = 13.75$, $r_F = 15.7$ and $b_J = 17.0$. These limits correspond to a median redshift around $15000 \, \mathrm{km \, s^{-1}}$. There are also additional targets drawn from various other optical, near-infrared, far-infrared, radio and X-ray catalogs. These additional target samples extend the science grasp and fully exploit the opportunity provided by the major hemispheric redshift survey. All the component samples in the z-survey, and the number of targets in each, are listed in Table 1.

The 6dFGS z-survey has a number of advantages over previous surveys. The sample is complete down to comparable limits in both optical and near-infrared (NIR) passbands. The NIR-selected subsamples are minimally affected by dust extinction within the Galaxy, allowing the sample to extend to within 10° of the Galactic plane. They are also little affected by dust extinction within the target galaxies themselves, so that, coupled with the fact that NIR luminosity is closely correlated with total stellar mass, these subsamples represent galaxies selected by stellar mass. Such samples are not biased towards the star-forming galaxies found in optical or far-infrared samples, which is both intrinsically preferable and also favors the selection of early-type galaxies suitable for D_n–σ measurements.

The v-survey sample is not distinct from the z-survey sample, nor do the observations differ. The v-sample simply comprises the subset of bright, early-type galaxies in the z-sample for which we obtain sufficiently high S/N spectra for measuring precise velocity dispersions and thus D_n–σ distances that are close to the intrinsic precision of the method (about 20%). Note that the measurements of D_n are based on the 2MASS images, and that the D_n–σ measurement errors are dominated by the errors on the velocity dispersions rather than the errors on D_n. We expect to obtain distances, and hence peculiar velocities, for about 15000 early-type galaxies within $15000 \, \mathrm{km \, s^{-1}}$.

2.   Science Goals

The goals of the 6dFGS z-survey include:

1. Measuring the luminosity function of NIR-selected galaxies (i.e. the stellar mass function of collapsed structures) and its variation with local environment and spectral type.

2. Mapping the local galaxy distribution (esp. close to the Galactic equator).

3. Quantifying the small- and large-scale clustering of galaxies weighted by stellar mass, and so constraining the scale-dependence of the biasing of the galaxies with respect to the dark matter.

4. Measuring the power spectrum of galaxy clustering on very large scales, comparable to the scales achieved by the 2dFGRS and SDSS.

5. Constructing a large, all-sky, volume-limited sample of early-type galaxies as the basis for the peculiar velocity survey.

6. Providing a fundamental redshift catalog for future work.

The goals of the 6dFGS v-survey include:

1. Mapping in detail the density and peculiar velocity fields over half the local volume to $\sim$15,000 km s^{-1}.

2. Providing additional constraints on cosmological models, and better measurements of fundamental parameters, from statistics of these fields.

3. Studying the ages, metallicities and star-formation histories of early-type galaxies over a wide range of masses and environments.

3.   Survey Details

The 6dFGS gets 175 dark or grey nights per year on the Anglo–Australian Observatory's 1.2m UK Schmidt Telescope, amounting to 75% of the available time on this telescope. The 6dF instrument itself is a multi-fiber spectrograph with 150 fibers covering a 6° diameter field of view (Watson et al. 2001). Each fiber has a projected diameter of 6.7″ on the sky, which is well-matched to the sizes of galaxies at redshifts around $z \sim 0.05$. The fibers are housed in removable field plate assemblies that can be mounted at the Schmidt focal plane or dismounted and placed in the 6dF robot for fiber re-positioning. There are currently two field plate assemblies, and in normal operation one field plate is configured on the robot while the other is in the telescope, thereby minimizing dead-time between fields.

The 10-m optical fibers feed a floor-mounted spectrograph which has a Marconi 1024^2 CCD with 13 μm pixels. The thinned CCD is back-illuminated and has a broad-band coating for enhanced blue sensitivity, which is as high as 75% even at 3900Å. The spectrograph currently has volume phase holographic (VPH) gratings, although in early survey observations reflectance gratings were
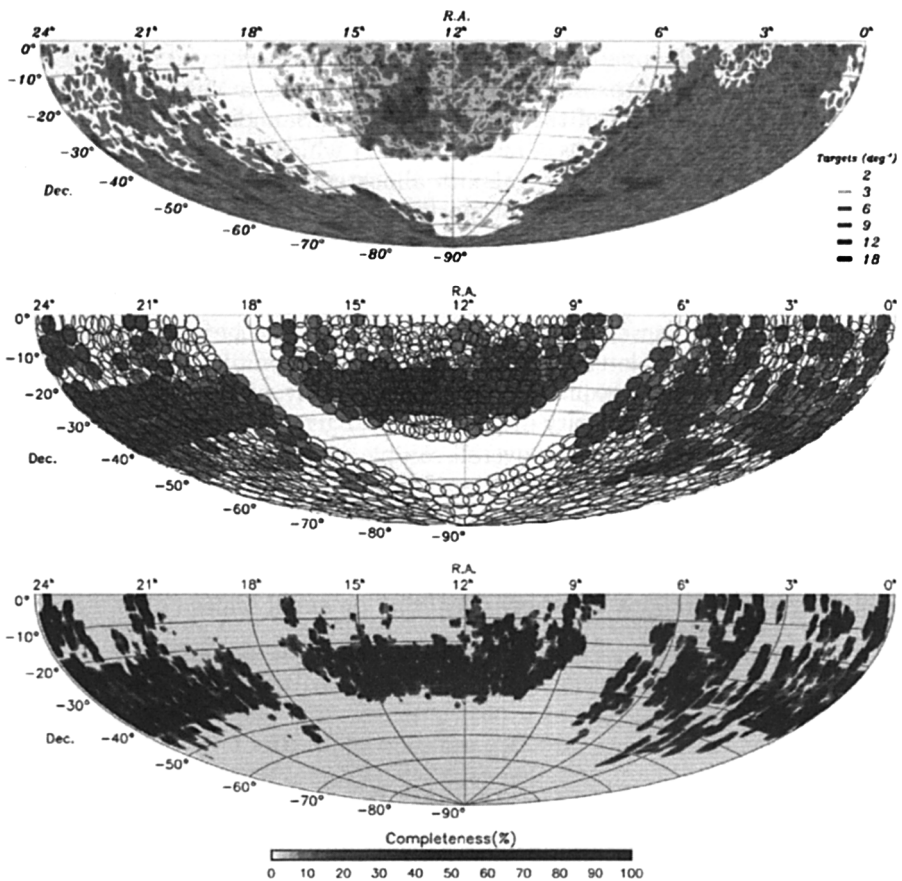
Figure 1.   The upper panel shows the surface density of targets in the 6dFGS. The middle panel shows the tiling of the sky with 6dF fields, and the observed (light grey) and redshifted (dark grey) fields as of June 2003. The lower panel shows the completeness as a function of position of the redshifts.

used; the VPH gratings have higher throughput, but otherwise both sets of gratings are similar. Survey observations for each field consist of 3×20 min exposures using the V grating and a 3×10 min exposures with the R grating; the V grating gives spectra with 5–6Å FWHM resolution over 4000–5600Å, while the R grating gives spectra with 9–12Å FWHM resolution over the range 5400–8400Å. Change-over of field plates and field acquisition take about 30 min, so that observing one field takes about 2 hours.

The density of the survey sample on the sky is shown in the upper panel of Figure 1. Because the NIR-selected sample favors early-type galaxies, which are more strongly clustered, and because the median redshift of the sample is relatively low compared to other large z-surveys (e.g. the 2dFGRS and SDSS surveys have median redshifts around $z = 0.1$), the projected distribution on the sky has much greater variance. Thus survey efficiency, and the completeness and

uniformity with which targets are observed, depend critically on the tiling of the sky with fields. High completeness and uniformity are achieved by covering the sky twice over with approximately 1500 6° fields, using a Metropolis algorithm to optimize the placement of the fields (Campbell, Saunders, & Colless 2004).

The algorithm maximizes a merit function which is computed as the sum over all fields of the number of galaxies allocated to fibers in each field, with each galaxy weighted by a factor proportional to $2^P n_6^{-1}$, where P is the target priority (see Table 1) and n_6 is the density of galaxies within a 6dF field centered on the galaxy. The priority weighting ensures that the primary and secondary samples are as complete as possible, at the expense of the additional target samples. The density weighting provides a compromise between achieving the maximum *overall* completeness and highly *uniform* completeness in each field. The Metropolis algorithm provides an effective way of optimizing this merit function despite the complexity of possible arrangements of fields.

The final tiling achieves an overall sample rate of 93.3%, an rms variation in the sampling uniformity of less than 5%, and an efficiency (in terms of the number of fibers assigned to galaxies in each field) of over 90%. Tests of the galaxies in the tiled sample shows that there are no significant sampling biases on large scales, but that the minimum fiber separation of 5.7′ leads to under-estimation of the amount of galaxy clustering on small scales ($<1\,h^{-1}\,$Mpc).

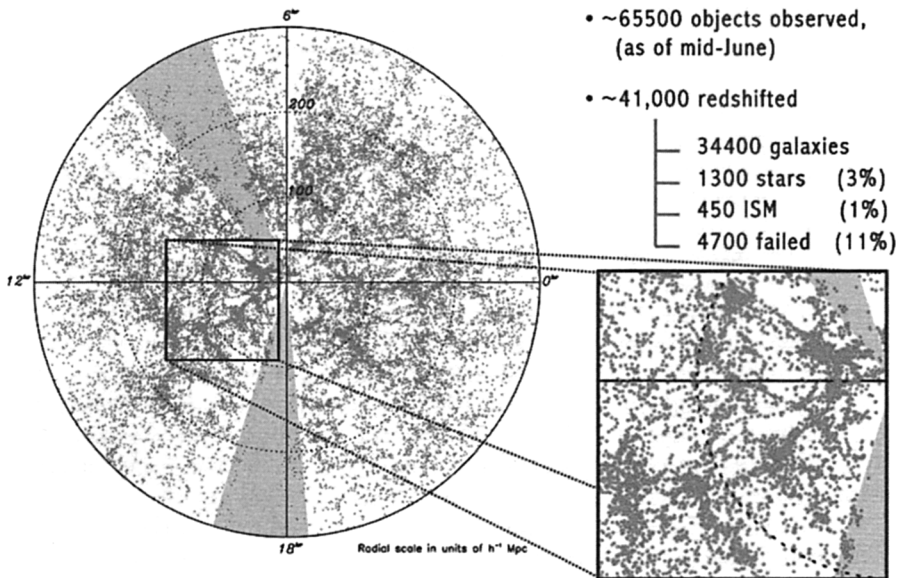## 4.   Status of the Survey

Figure 2.   The distribution of galaxies with redshifts measured up to June 2003, as viewed from the south Galactic pole. The inset shows the level of detail in the large scale structures revealed by the 6dFGS.

As at mid-June 2003, 651 of the 1500 survey fields (43%) have been observed, and at the present rate of progress the survey is on target for completion in mid-2005. The intention is to cover the sky in thirds (although observational expediency means that these priorities cannot be strictly adhered to): first a central declination strip, $-42° < \delta < 22°$, then an equatorial strip, $-22° < \delta < 0°$, and finally the southern polar cap, $\delta < -42°$. The middle panel of Figure 1 shows the tiling of the sky with 6dF fields; the 651 fields observed up to mid-June are shaded, with the 415 fields in which redshifts have been measured in a darker shading. The lower panel of the figure shows the redshift completeness of the sample on the sky for the 65500 objects observed to date.

Of the 41000 objects for which redshifts have been measured so far, 34400 are galaxies (84%), 1300 (3%) are stars, 450 (1%) are ISM emission line regions, and 4700 (11%) are unidentified. Figure 2 shows the 34400 galaxies with redshifts projected in the declination–redshift plane.

5. Cosmological constraints from the 6dFGS

The fundamental cosmological parameters are already quite well-constrained by a wide range of existing large-scale structure datasets: the 2dFGRS and SDSS galaxy redshift surveys, the WMAP CMB anisotropy measurements, the distances to high-redshift SNe, the clustering of the Lyman α forest, and the weak lensing of galaxies. Given this plethora of data, what can the 6dFGS add? Specifically, what advantage does the combination of redshift and peculiar velocity information give?

The answers presented here come from the work of Burkey & Taylor (2004), who have analyzed the Fisher information matrices for the z- and v-surveys, both individually and combined.

In this study the parameters used to specify the cosmological model, and in particular the relationship between the mass and galaxy distributions, are: (1) the amplitude of the galaxy power spectrum, which is related to the amplitude of the mass power spectrum by the bias parameter, $A_g = bA_m$; (2) the amplitude of the velocity field $A_v = \Omega^{0.6}A_m$; (3) the power spectrum shape parameter, $\Gamma = \Omega_m h$; (4) the mass density in baryons, $\omega_b = \Omega_b h$; (5) the redshift-space distortion parameter, $\beta = \Omega_m^{0.6}/b$; and (6) the correlation coefficient between luminous and dark matter, r_g.

The fiducial model assumes a cold dark matter power spectrum with primordial index $n = 1$ and has fundamental physical parameters $(A_m, h, \Omega_m, \omega_b, b, r_g) = (5 \times 10^{-5}, 0.65, 0.3, 0.025, 1, 1)$, which correspond to the measurable parameters $(A_g, A_v, \Gamma, \omega_b, \beta, r_g) = (5 \times 10^{-5}, 2.4 \times 10^{-5}, 0.195, 0.025, 1, 1)$.

There are several degeneracies between these parameters, as can be seen by comparing derivatives of the galaxy and velocity logarithmic power spectra with respect to the various parameters as functions of wavenumber; similar functional shapes mean almost degenerate parameters: A_g, β, and r_g are all approximately constant and so approximately degenerate (they all affect the normalization of the power spectrum); Γ and ω_b are also similar (both damp the power spectrum), and the effective shape is $\Gamma_{\text{eff}} = \Gamma \exp(-2\Omega_b h)$.
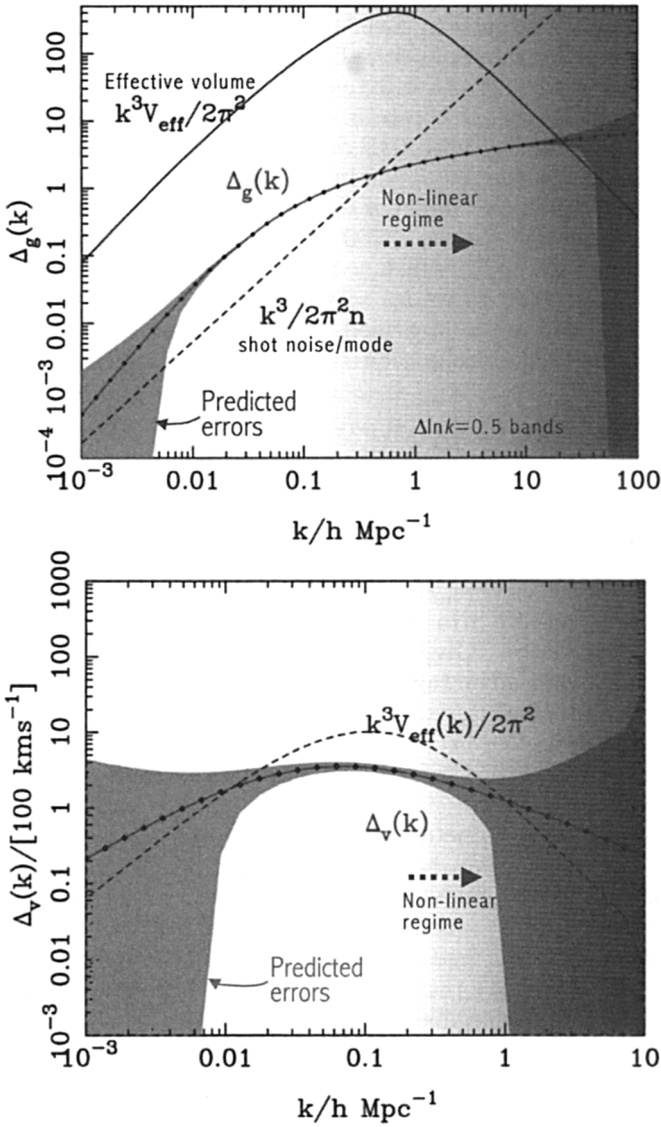
Figure 3.   The upper panel shows the predicted precision of the band-averaged redshift-space linear power spectrum of the galaxy distribution recovered from the 6dFGS z-survey; also the effective survey volume and the shot-noise per mode. The lower panel shows the predicted precision of the peculiar velocity power spectrum, $\Delta_v(k) = (k^3 P_v(k)/2\pi^2)^{1/2}$, recovered from the 6dFGS v-survey; also the effective survey volume. The increasing effect of non-linear evolution on the power spectra is indicated by the increasing shading at larger wavenumbers. (Burkey & Taylor 2004)
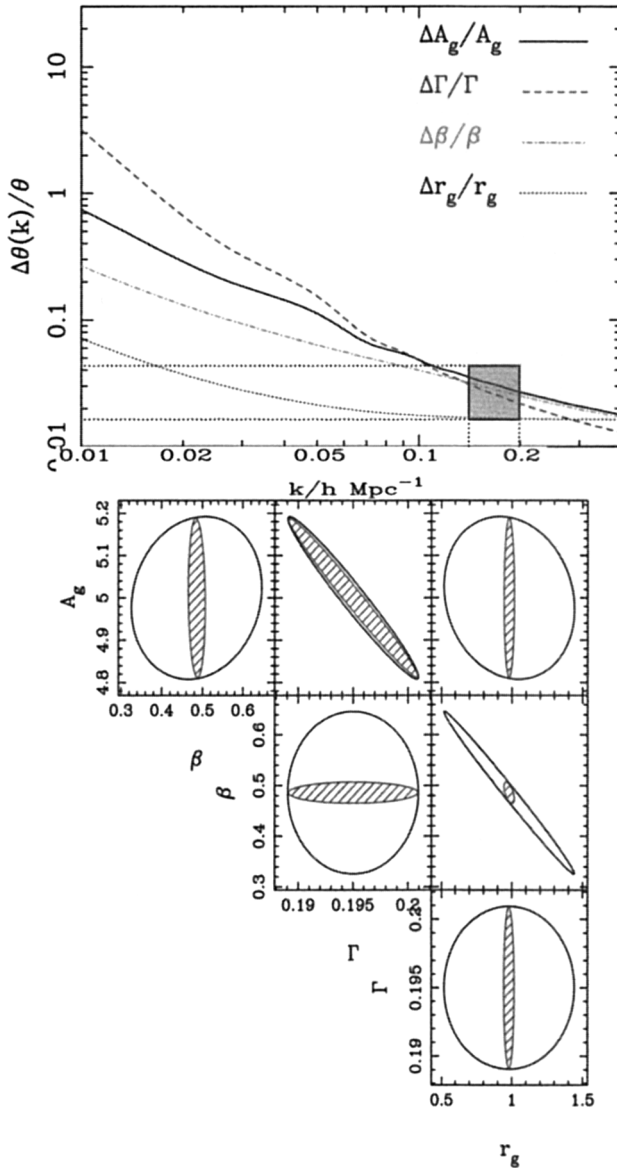
Figure 4. The upper panel shows, as a function of limiting wavenumber (imposed by non-linearity), the predicted precision of the various parameters determined from the combined $z + v$-survey in a four-parameter model involving A_g, Γ, β and r_g; the box shows the expected range of uncertainties. The lower panels show, for the z-survey alone (open ellipses) and for the combined $z + v$-surveys (hatched ellipses), the expected 1σ constraints on various pairs of parameters; note the significant gains from adding the peculiar velocity v-survey. (Burkey & Taylor 2004).
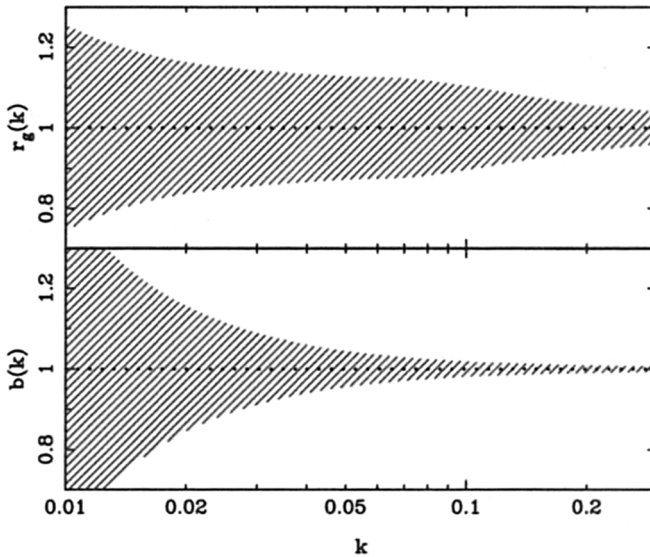
Figure 5.   The errors on band estimates of r_g and b from the combined $z+v$-survey, in each case assuming the other is held fixed. (Burkey & Taylor 2004).

The upper panel of Figure 3 shows the expected precision with which the redshift-space galaxy power spectrum will be recovered from the 6dFGS z-survey. Using the z-survey alone, the Fisher matrix analysis indicates that A_g, Γ and β can recovered with errors of about 3%. However the uncertainties on ω_b and r_g are much larger, due to the strong correlations between ω_b and Γ (and A_g) and between β and r_g.

While a larger redshift survey (like the 2dFGRS or SDSS) can achieve tighter constraints on these parameters, the 6dFGS offers the unique opportunity to combine the redshift-space galaxy power spectrum with the velocity power spectrum. The expected errors on the 3D velocity power spectrum derived from the 6dFGS v-survey are shown in the lower panel of Figure 3. The errors on the velocity power spectrum are larger than the errors on the galaxy power spectrum, reflecting in part the smaller sample size of the v-survey and in part the fact that only 1D radial velocities are available for each galaxy (as opposed to 3D redshift-space positions).

The value of the v-survey is that it helps break some of the degeneracies between parameters that are present in the z-survey. When the Fisher matrix analysis is applied to the combined $z+v$-survey constraints (i.e. both the galaxy and velocity power spectra), models specified by A_g, Γ, β and r_g have errors in all four parameters of only 2–3% (see Figure 4). Adding the v-survey greatly improves the joint constraints on β and r_g, which are now only relatively weakly correlated.

Another question of great importance for theories of galaxy formation is the extent to which the bias, or the galaxy–mass correlation coefficient, varies with scale. Figure 5 shows the errors on band estimates of r_g and b from the

$z + v$-survey as a function of scale (in each case assuming the other parameter is fixed). If b is fixed, variations in r_g can be measured at 5-10% level; if r_g is fixed, variations in b can be measured at the few % level over a wide range of scales.

References

Burkey, D., & Taylor, A. N. 2004, MNRAS, 347, 255

Campbell, L., Saunders, W., & Colless, M. 2004, MNRAS, 350, 1467

Jarrett, T. H., et al. 2000a, AJ, 119, 2498

Jarrett, T. H., et al. 2000b, AJ, 120, 298

Parker, Q. A., Colless, M., & Mamon, G. 1997a, PASA, 14, 125

Parker, Q. A., Colless, M., & Mamon, G. 1997b, in ASSL Vol. 212, Wide-Field Imaging, ed. E. Kontizas, M. Kontizas, D. H. Morgan & G. P. Vettolani (Dordrecht: Kluwer), 303

Wakamatsu, K., et al. 2003, in ASP Conf. Ser. Vol. 289, IAU 8th Asia-Pacific Regional Meeting, ed. S. Ikeuchi, J. Hearnshaw, & T. Hanawa (San Francisco: ASP), 97, astro-ph/0306104

Watson, F.G., et al. 2001, in ASP Conf. Ser. Vol. 232, A New Era in Wide-Field Astronomy, ed. R. Clowes, A. Adamson & G. Bromage (San Francisco: ASP), 421